JOURNAL OF MORPHOLOGY 211:95–118 (1992)

Cranial Ontogeny in the Direct-Developing Frog, *Eleutherodactylus coqui* (Anura: Leptodactylidae), Analyzed Using Whole-Mount Immunohistochemistry

JAMES HANKEN, MICHAEL W. KLYMKOWSKY, CLIFF H. SUMMERS, DANIEL W. SEUFERT, AND NICOLE INGEBRIGTSEN
Department of Environmental, Population, and Organismic Biology (J.H., N.I., D.W.S.), and Department of Molecular, Cellular, and Developmental Biology (M.W.K.), University of Colorado, Boulder, Colorado 80309; Department of Biology, University of South Dakota, Vermillion, South Dakota 57069 (C.H.S.)

ABSTRACT Direct development in amphibians is an evolutionarily derived life-history mode that involves the loss of the free-living, aquatic larval stage. We examined embryos of the direct-developing anuran *Eleutherodactylus coqui* (Leptodactylidae) to evaluate how the biphasic pattern of cranial ontogeny of metamorphosing species has been modified in the evolution of direct development in this lineage. We employed whole-mount immunohistochemistry using a monoclonal antibody against the extracellular matrix component Type II collagen, which allows visualization of the morphology of cartilages earlier and more effectively than traditional histological procedures; these latter procedures were also used where appropriate. This represents the first time that initial chondrogenic stages of cranial development of any vertebrate have been depicted in whole-mounts.

Many cranial cartilages typical of larval anurans, e.g., suprarostrals, cornua trabeculae, never form in *Eleutherodactylus coqui*. Consequently, many regions of the skull assume an adult, or postmetamorphic, morphology from the inception of their development. Other components, e.g., the lower jaw, jaw suspensorium, and the hyobranchial skeleton, initially assume a mid-metamorphic configuration, which is subsequently remodeled before hatching. Thirteen of the adult complement of 17 bones form in the embryo, beginning with two bones of the jaw and jaw suspensorium, the angulosplenial and squamosal. Precocious ossification of these and other jaw elements is an evolutionarily derived feature not found in metamorphosing anurans, but shared with some direct-developing caecilians. Thus, in *Eleutherodactylus* cranial development involves both recapitulation and repatterning of the ancestral metamorphic ontogeny. These modifications, however, are not associated with any fundamental change in adult morphology and cannot at this time be causally linked to the evolutionary success of this extraordinarily speciose genus.

Direct development in amphibians is a life-history mode that involves the evolutionary loss of the free-living larval stage characteristic of metamorphosing taxa. It has evolved repeatedly in all three extant orders and characterizes the majority of species in some lineages (Duellman and Trueb, '86; Wake, '89). By comparing direct developers with related metamorphosing taxa, it is possible to examine fundamental questions concerning both mechanistic and evolutionary aspects of development. These include the developmental basis of homology, the evolution of developmental pathways and mechanisms for pattern formation and morphogenesis, and the existence and mode of action of developmental constraints on morphological diversification (Elinson, '90; Elinson et al., '90; Hanken, '89; Raff, '87; Wake and Roth, '89). Yet, at least in amphibians, direct development has been investigated primarily from ecological and life-history perspectives (e.g., Altig and Johnston, '89; Duellman, '89; McDiarmid, '78); there are few comprehensive studies of

the *developmental* basis of direct development in any species.

The present paper is the first in a projected series of studies of the cranial ontogeny in the direct-developing leptodactylid frog *Eleutherodactylus coqui*. We focus on the skull and associated tissues because of (1) the dramatic morphological transformation that these tissues undergo in metamorphosing taxa, especially anurans (Hanken and Hall, '88a,b; Hanken and Summers, '88a), and (2) the key role that cranial tissues, and especially trophic and respiratory structures, play in the adaptive diversification of many amphibian lineages (Wake and Roth, '89). *Eleutherodactylus* was chosen for several reasons. First, its ontogeny is among the most derived of any direct-developing anuran with respect to the ancestral biphasic pattern of development found in metamorphosing taxa. Indeed, it is widely regarded as the least recapitulatory, in terms of the presence of larval structures, of any direct-developing frog (Elinson, '90; Hanken et al., '90; Hanken and Summers, '88b; Hughes, '65, '66; Lynn, '61; Orton, '51). Second, embryos of the Puerto Rican species *E. coqui* are readily obtained from laboratory breeding colonies (Elinson et al., '90). Third, as the most speciose genus of terrestrial vertebrates (ca. 450 species are described at present, Hedges, '89), *Eleutherodactylus* provides an opportunity to evaluate hypotheses concerning the evolutionary significance of derived developmental patterns (sensu Lauder and Liem, '89). Until now, these hypotheses have been based primarily on the examination of other groups; e.g., ontogenetic repatterning in plethodontid salamanders (Roth and Wake, '89; Wake and Roth, '89).

We do not provide a comprehensive account of all aspects of cranial development in *Eleutherodactylus coqui*. Rather, we focus on those features that undergo the most dramatic transformation between larval and adult stages in metamorphosing taxa. These include the cartilaginous components of the lower jaw and jaw suspensorium, the hyobranchial skeleton, and the anterior neurocranium, as well as the ossification sequence. We have employed a new technique for whole-mount immunohistochemistry (Dent et al., '89; Dent and Klymkowsky, '89) using a monoclonal antibody against the extracellular matrix component Type II collagen. This technique allows visualization of the morphology of cartilages during initial stages of their development more effectively than traditional histological procedures, e.g., Alcian blue–stained whole-mounts and serial sections, and leaves virtually no technical artifacts (reviewed in Klymkowsky and Hanken, '91). Because this represents the first time that whole-mount immunohistochemistry has been applied to the study of skeletal development in amphibians, we also include brief descriptions of the postcranial skeleton at each stage in order to help put the pattern of cranial development in the context of skeletogenesis overall and to supplement criteria for staging embryos. Our primary objectives are (1) to evaluate how and to what extent the characteristic biphasic pattern of cranial development in metamorphosing taxa has been modified during the evolution of direct development in *Eleutherodactylus coqui* and (2) to explore the implications of these results concerning the developmental mechanisms for morphological evolution in amphibians, as well as other taxa with complex life cycles (e.g., echinoderms—Raff, '87).

MATERIALS AND METHODS

Animal care

Embryonic and early posthatching specimens of *Eleutherodactylus coqui* were obtained primarily from spontaneous matings among wild-caught adults maintained as a laboratory breeding colony (Elinson et al., '90). A few clutches were collected in the field (El Verde Field Station, Luquillo Experimental Forest, Puerto Rico) following natural matings; the eggs were reared in the laboratory in Boulder. Once removed from the attending male, eggs were separated, briefly immersed in antibiotic (5 mg gentamicin sulfate per 100 ml 10% Holtfreter's solution), and placed atop 100 gm sterile sand moistened with 5–6 ml deionized water in glass petri dishes (Taigen et al., '84). Eggs in closed dishes were incubated in the dark at 23°C and removed and preserved periodically. Newly hatched froglets were maintained at room temperature on moistened filter paper in glass petri dishes and fed wingless fruitflies ad libitum.

Staging and terminology

Embryonic stages were determined according to the table provided by Townsend and Stewart ('85). Anatomical terminology follows that advocated by Duellman and Trueb ('86), except as otherwise noted.

Histology

Two kinds of whole-mounts were prepared—one using traditional methods for vi-

sualizing skeletal tissues, the other using immunohistochemistry (Table 1). For traditional preparations, specimens were fixed and preserved in 10% neutral-buffered formalin (NBF; Humason, '79) and differentially stained for bone (alizarin red) and cartilage (Alcian blue) by using standard procedures (Dingerkus and Uhler, '77; Hanken and Wassersug, '81). For whole-mount immunohistochemistry (Dent and Klymkowsky, '89; Dent et al., '89; Klymkowsky and Hanken, '91), specimens were fixed overnight in Dent fixative (1 part DMSO, dimethyl sulfoxide: 4 parts methanol) and then bleached in a solution of 1 part 30% hydrogen peroxide: 2 parts Dent fixative for 2–5 days. Investing jelly coats were removed manually, after which specimens were incubated at room temperature with a monoclonal antibody against Type II collagen ($II_6B3/15A4$; Linsenmayer and Hendrix, '80) diluted 1:100 into bovine calf serum supplemented with 5% DMSO and then incubated with an affinity-purified, peroxidase-conjugated, goat anti-mouse antibody (BioRad). After reaction with diaminobenzidine, specimens were dehydrated and cleared in BABB (1 part benzyl alcohol: 2 parts benzyl benzoate).

Additional specimens preserved in either NBF or Smith fixative (Humason, '79) were prepared as 8–10-μm serial sections differentially stained for connective tissues by using Alcian blue, direct red, celestine blue, and hematoxylin (Hall, '85).

Microscopy and photomicrography

Specimens were examined by using either a Wild M8 (whole-mounts) or a Leitz Dialux 22 (serial sections) microscope. Angles were measured in whole-mounts by using an ocular protractor. Orientation of the palatoquadrate was defined as the angle, in lateral view, between the floor of the neurocranium and the long axis of the palatoquadrate defined by the articular and otic processes (Wassersug and Hoff, '82). Photographs were made on Kodak T-Max film (EI 100 or 400) by using a Wild MPS55 Photoautomat and tungsten illumination, plus a Wratten No. 8 (yellow) filter.

TABLE 1. Specimens examined

Townsend–Stewart stage	Serial sections	Whole-mounts	
		Alcian–alizarin	Collagen
5	—	—	2
6	2	—	2
7	5	—	2
8	3	—	2
9	1	—	1
10	1	2	3
11	1	2	3
12	1	4	3
13	1	5	3
14	1	5	3
15	2	5	2
15+[1]	1	15	—

[1]Preserved within 2 mo after hatching; mean snout-vent length equals 8.4 mm (range 6.8–10.1).

RESULTS

Cartilaginous skull

Cartilage development is described primarily from whole-mounts (Table 1). Immunostained preparations are effective for describing individual cartilages as early as Stage 7, and prechondrogenic events at even earlier stages. Alizarin-red-Alcian-blue-stained preparations are effective for Stages 10 and higher, yet immunostained preparations often provide greater resolution and give more consistent results at the same stages. Serial sections are used to examine prechondrogenic condensations and to resolve specific questions concerning structure, timing, and degree of fusion.

Prechondrogenic stages (Townsend-Stewart, T-S 5–6)

Stage 5 (Figs. 1A,B, 2A,B). Collagen-rich areas are limited to the notochordal sheath and the otic vesicles, and intersegmental boundaries along the trunk and the first two or three caudal segments. The notochord, which is well stained along its entire length, extends from a point just anterior to the otic vesicles to the tip of the tail.

Stage 6. Whole-mounts at this stage closely resemble those from Stage 5. In sections, prechondrogenic condensations are beginning to form, e.g., surrounding otic vesicles, but these are not yet Alcian blue–positive.

Chondrogenic stages (T-S 7–15)

Stage 7 (Fig. 2C,D). Cartilage is evident for the first time. In immunostained whole-mounts, the notochord is still deeply stained at its rostral tip and in the tail; the trunk portion is fainter. In general, intersegmental boundaries are fainter except for the neural arches, which first appear as paired rods on either side of the neural tube. The femur, tibia, and fibula are visible for the first time; distal hind limb and all forelimb cartilages cannot be seen.

In the head, paired cranial trabeculae are visible both in whole-mounts and serial sec-

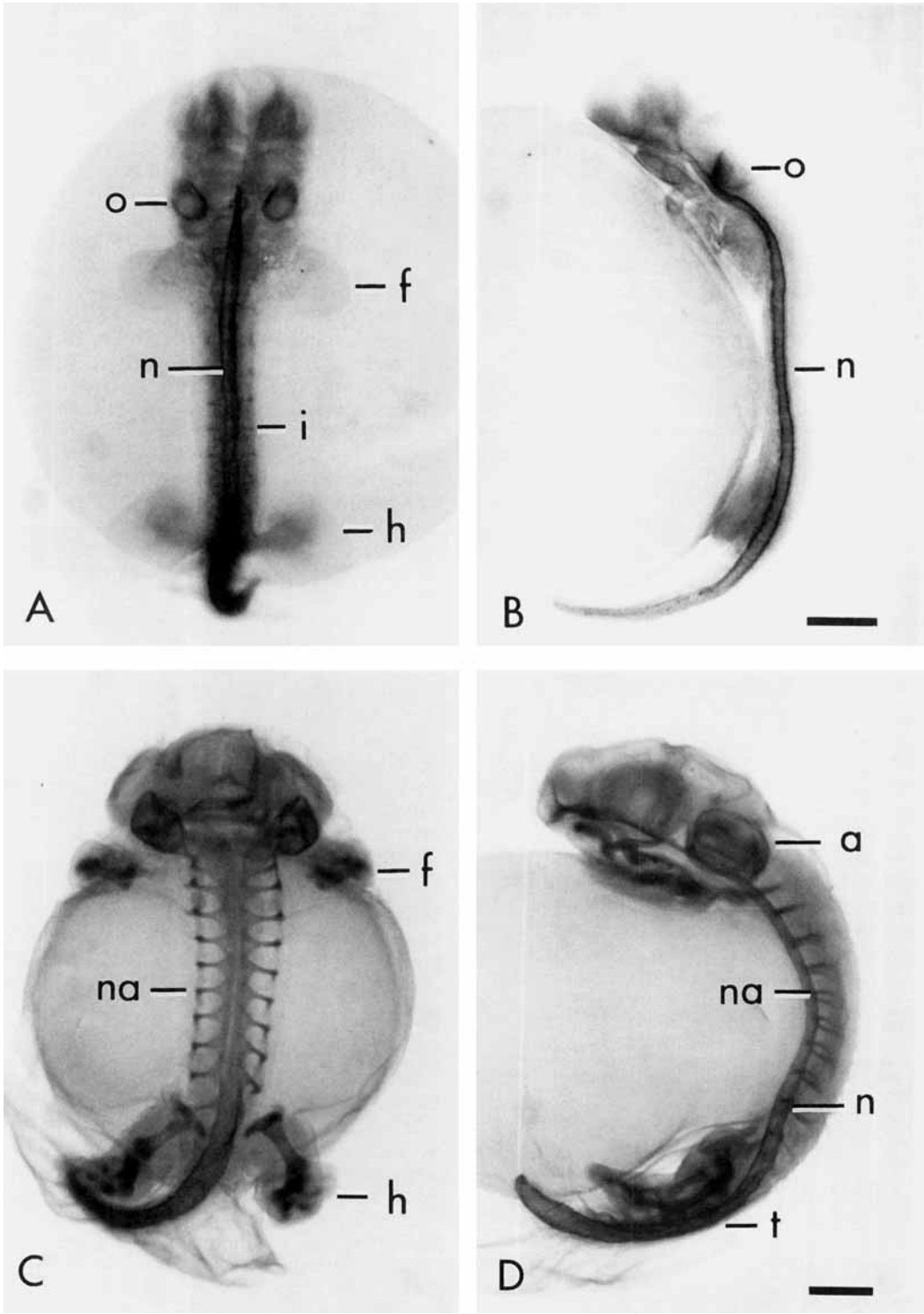

Figure 1

tions (Fig. 2C,D). Each is represented by a thin, longitudinal rod of cartilage that lies ventromedial to the eye and ventrolateral to the brain. They are united posteriorly, but anterior to the notochord, by a thin, transverse sheet of cartilage (hypochordal commissure) that is the rudimentary basal plate. No other cranial cartilages are visible, although there are two transverse, collagen-rich bands in the ventral portion of the head at the level of the eyes. In sections, these bands correspond to the prechondrogenic condensations of the developing mandible and hyobranchial skeleton. The formerly spherical otic vesicles are beginning to assume the complex form of the membranous labyrinths. Collagen staining is dense at the periphery of each vesicle, corresponding to the prechondrogenic condensations of the auditory capsules which still are Alcian blue–negative.

Stage 8 (Fig. 2E,F). Hind-limb cartilages are visible proximal to the metatarsals, as are forelimb cartilages proximal to the manus. Neural arches are distinct; they first extend transversely from the notochord and then curve dorsally around the neural tube.

In the head, cranial trabeculae approach one another rostrally but remain separated by a wide gap (Fig. 2E). Suprarostral cartilages and cornua trabeculae are absent and never form. A pair of delicate cartilaginous pillars—pila antotica and pila metoptica—ascend dorsally from each cranial trabecula on either side of the braincase medial to the eyes (not visible in figures). Auditory capsular cartilage is distinct and Alcian blue–positive for the first time. A prominent nodule of calcified endolymph is present dorsal to each auditory capsule. Paired mandibular cartilages are "L-shaped" in dorsal view; transverse arms (infrarostral cartilages) articulate anteromedially; longitudinal arms (Meckel's cartilages) extend posterolaterally to articulate with the palatoquadrate cartilages. The rod-shaped palatoquadrate cartilage is located anterior to the auditory capsule. From its posterodorsal tip (otic process), it descends anteroventrally at an angle of 35° below the floor of the neurocranium to its articulation with Meckel's cartilage beneath the orbit. It is separate from the neurocranium and lacks a commissura quadratocranialis anterior (de Beer, '37), muscular process, and ascending process, none of which ever forms. In terms of their overall shape, degree of fusion, and the location of the jaw joint, Meckel's, infrarostral, and palatoquadrate cartilages resemble a mid-metamorphic stage of development in metamorphosing anurans (e.g., *Bombina orientalis,* Hanken and Summers, '88a; Fig. 2C,D).

The hyobranchial skeleton comprises a continuous ventral mass of cartilage that, in dorsal view, lies between the eyes and auditory capsules (Figs. 2E,F, 6). A longitudinal series of four paired processes extends laterally from the central region (hypobranchial plate). The most anterior process is largest and resembles the ceratohyal cartilage of larval frogs; the remaining processes (ceratobranchials I–III) are progressively thinner, shorter, and fainter from anterior to posterior. All three ceratobranchials are rod-shaped and lack any of the secondary or tertiary branching characteristic of these cartilages in larval frogs (cf. Hanken and Summers, '88a; Figs. 1A, 2A,B).

Stage 9 (Figs. 1C,D, 3A,B). Fore- and hind-limb cartilages are distinct from the limb girdles to the proximal phalanges. The notochord is collagen-rich along its entire length, but especially in the tail. Neural arches remain slender rods; the dorsal tips are now slightly curved posteriorly.

Rostrally, cranial trabeculae are joined by a transverse rod of cartilage—the trabecular plate (Fig. 3A,B). Paired flanges descend ventrally from this cartilage; eventually, they will form the floor of each nasal capsule, the solum nasi. A lateroventral rod of cartilage—the lamina orbitonasalis (= planum antorbitale of the adult)—emerges from each cranial trabecula at the anterior margin of the orbital region; the preoptic root, which forms the anterolateral corner of the braincase, also arises dorsally from this point. Pilae antotica and metoptica on either side are joined dorsally by the developing orbital cartilages me-

Fig. 1. Immunostained whole-mounts of *Eleutherodactylus coqui* in dorsal (**A,C**) and lateral (**B,D**) views, depicting the distribution of Type II collagen before and after the inception of chondrogenesis. At T-S Stage 5 (A,B), positive staining for collagen is limited to dark areas of the notochordal sheath, otic vesicles, and intersegmental boundaries of the trunk, and the proximal portion of the tail. Additional gray areas represent nonspecific background staining. At T-S Stage 9 (C,D), positive staining denotes cartilage, with the principal exception of the notochordal sheath, which is still nonchondrogenic. Abbreviations: a, auditory capsule; f, forelimb; h, hind limb; i, intersegmental boundaries; n, notochord; na, neural arch; o, otic vesicle; t, tail. Scale is the same for each horizontal pair of photographs; scale bars = 0.5 mm.

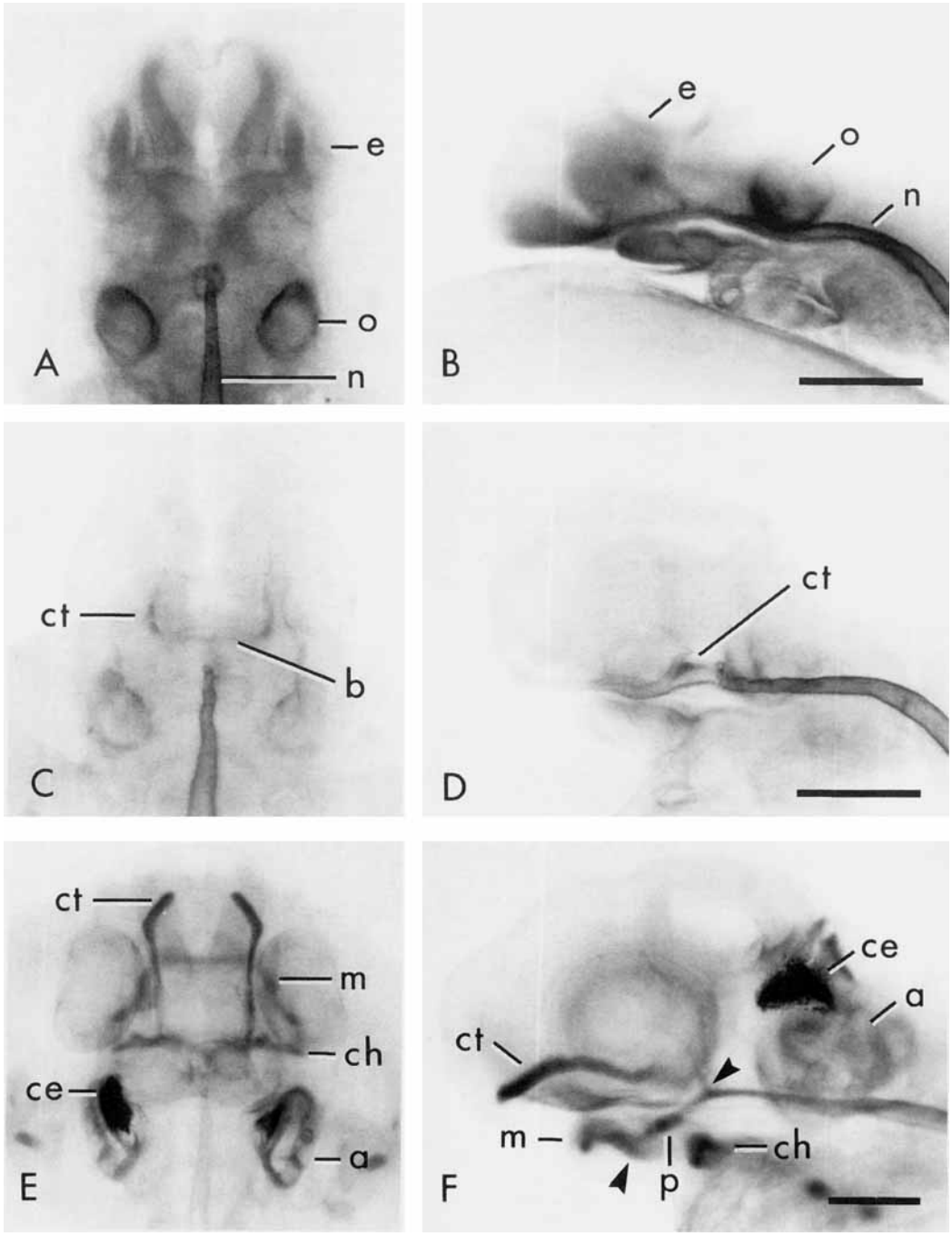

Fig. 2. Immunostained whole-mounts of *Eleutherodactylus coqui* depicting cranial development at T-S Stages 5 (**A,B**), 7 (**C,D**), and 8 (**E,F**). Each stage is depicted in dorsal (**left panel**) and lateral (**right panel**) views. Arrowheads in F denote dorsal otic and ventral articulating processes of the palatoquadrate cartilage (p). Additional abbreviations: b, basal plate; ce, calcified endolymph; ch, ceratohyal; ct, cranial trabecula; e, eye; m, mandible. Scale is the same for each horizontal pair of photographs; scale bars = 0.5 mm.

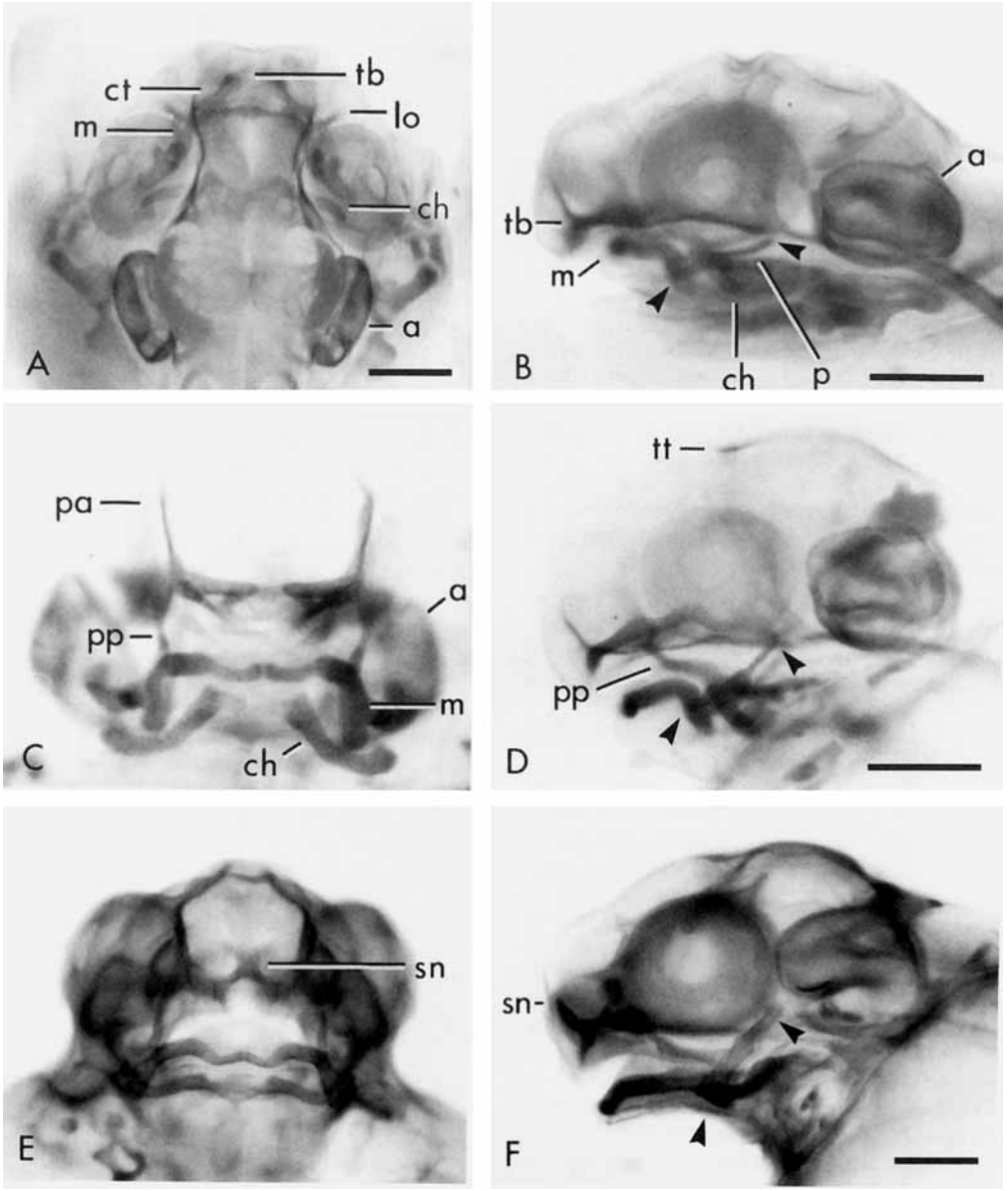

Fig. 3. Immunostained whole-mounts of *Eleutherodactylus coqui* depicting cranial development at T-S Stages 9 (**A,B**), 10 (**C,D**), and 11 (**E,F**). Each stage is depicted in dorsal or anterior (**left panel**) and lateral (**right panel**) views. Arrowheads as in Figure 2. Additional abbreviations: lo, lamina orbitonasalis; pa, pila antotica; pp, pterygoid process of palatoquadrate; sn, septum nasi; tb, trabecular plate; tt, taenia tecti transversalis. Scale is the same for each horizontal pair of photographs unless indicated otherwise; scale bars = 0.5 mm.

dial to the eyes to form the braincase walls, which are lined with prominent, C-shaped nodules of calcified endolymph anteromedial to the auditory capsules. The mandible is longer and thinner than in Stage 8, with a shallower angle between transverse and longitudinal arms on each side. It is largely oriented in the frontal plane, except at the articulation with the palatoquadrate cartilage where it is deflected ventrally. The pala-

toquadrate is oriented as in Stage 8 and remains well separated from the braincase. At the midpoint of the palatoquadrate, there is a ventral articulation with the ceratohyal cartilage. Dorsal to this articulation, a prominent pterygoid process extends first medially and then anteriorly, closely following the curvature of the adjacent mandible, until it ascends to fuse with the braincase via the posterior maxillary process of the lamina orbitonasalis.

The hyobranchial skeleton is different from that of Stage 8 (Fig. 6). The hypobranchial plate is larger relative to ceratobranchials I–III, and ceratobranchial IV is visible as a tiny transverse process emerging on either side from the posterolateral margin of the hypobranchial plate. The long axis of each ceratohyal has become obliquely oriented as the lateral articulation with the palatoquadrate has migrated posteriorly.

Stage 10 (Fig. 3C,D). Notochord and vertebrae are as in Stage 9; dorsal, recurved tips of neural arches extend farther posteriorly. All limb cartilages are distinct, including distal phalanges.

The neurocranium is more robust (Fig. 3C,D). Trabecular and basal plates are more extensive, and the septum nasi, which forms initially as a transverse sheet of cartilage, separates the developing nasal capsules (cf. Fig. 3E,F). A thin, transverse band of cartilage, the taenia tecti transversalis, forms a dorsal bridge over the braincase immediately anterior to the pila metoptica. Paired nodules of calcified endolymph closely follow the walls of the braincase medial to the auditory capsules and approach one another posteriorly. The mandible is more elongate; the jaw articulation has advanced caudally to a level immediately anterior to the optic foramen. As in earlier stages, each side of the mandible comprises a single, continuous, cartilaginous rod. However, thin, crescentic, anteromedial segments resemble the infrarostral cartilages of metamorphosing anuran larvae, and in this way they are distinct from laterally adjacent segments (Meckel's cartilage) (Fig. 3C). The palatoquadrate is more upright (40°); the otic process approaches, but remains separate from, the anterior border of the auditory capsule.

The hyobranchial skeleton has continued to diverge from its initial form (Fig. 6). The ceratohyal is more prominent and elongate; its primary axis forms an angle of approximately 60° with the long axis of the skull. Ceratobranchial I is as long as, and oriented parallel to, the ceratohyal, but it tapers distally. Ceratobranchial (CB) II is much smaller than CB I and is oriented transversely. Ceratobranchials III and IV are slightly shorter than CB II and emerge from the hypobranchial plate by a common stalk before separating after about one-half their length; they are oriented slightly posterolaterally.

Stage 11 (Fig. 3E,F). Collagen staining of the notochord is faint in the head and trunk but still prominent in the tail. Neural arches bear prominent anterior and posterior processes, corresponding to the pre- and postzygapophyses. The third presacral vertebra (second behind the atlas) bears an anterolateral process that approaches the shoulder girdle. The craniovertebral articulation is established. All limb cartilages are distinct.

The neurocranium is well developed (Fig. 3E,F). Nasal capsular cartilages, in particular, are more extensive; tectum nasi, solum nasi, and planum terminale are distinct. Nodules of calcified endolymph within the braincase are still prominent, but they are asymmetrical and more widely separated posteriorly than at earlier stages. The mandible is more robust and elongate; the jaw articulation lies ventral to the optic foramen. Anteromedial segments remain thinner than lateral segments (Figs. 3E, 7A). The palatoquadrate is more stout and upright in lateral view (50°), but it retains a solid connection with the neurocranium via the pterygoid process. The otic process remains separate from the neurocranium. The palatoquadrate at this stage resembles that of a mid-metamorphic *Rana* depicted by de Beer ('37; Pl. 75, Fig. 3).

The hyobranchial skeleton is prominent and beginning to resemble the hyale of a metamorphosed froglet (Fig. 6). The ceratohyal is longer and more sinuous; the anterior processes are rudimentary. Ceratobranchial I is nearly as long as the ceratohyal, but its distal half is now much thinner than the base. Ceratobranchials II–IV are much thinner and shorter than CB I and the ceratohyal.

Stage 12 (Fig. 4A,B). Immunostaining of the notochord is similar to that at Stage 11. Vertebrae are better developed. Opposing neural arches are beginning to arch over the neural tube and approach one another, although they still are widely separated. In the trunk, anterior and posterior processes that correspond to the future pre- and postzyg-

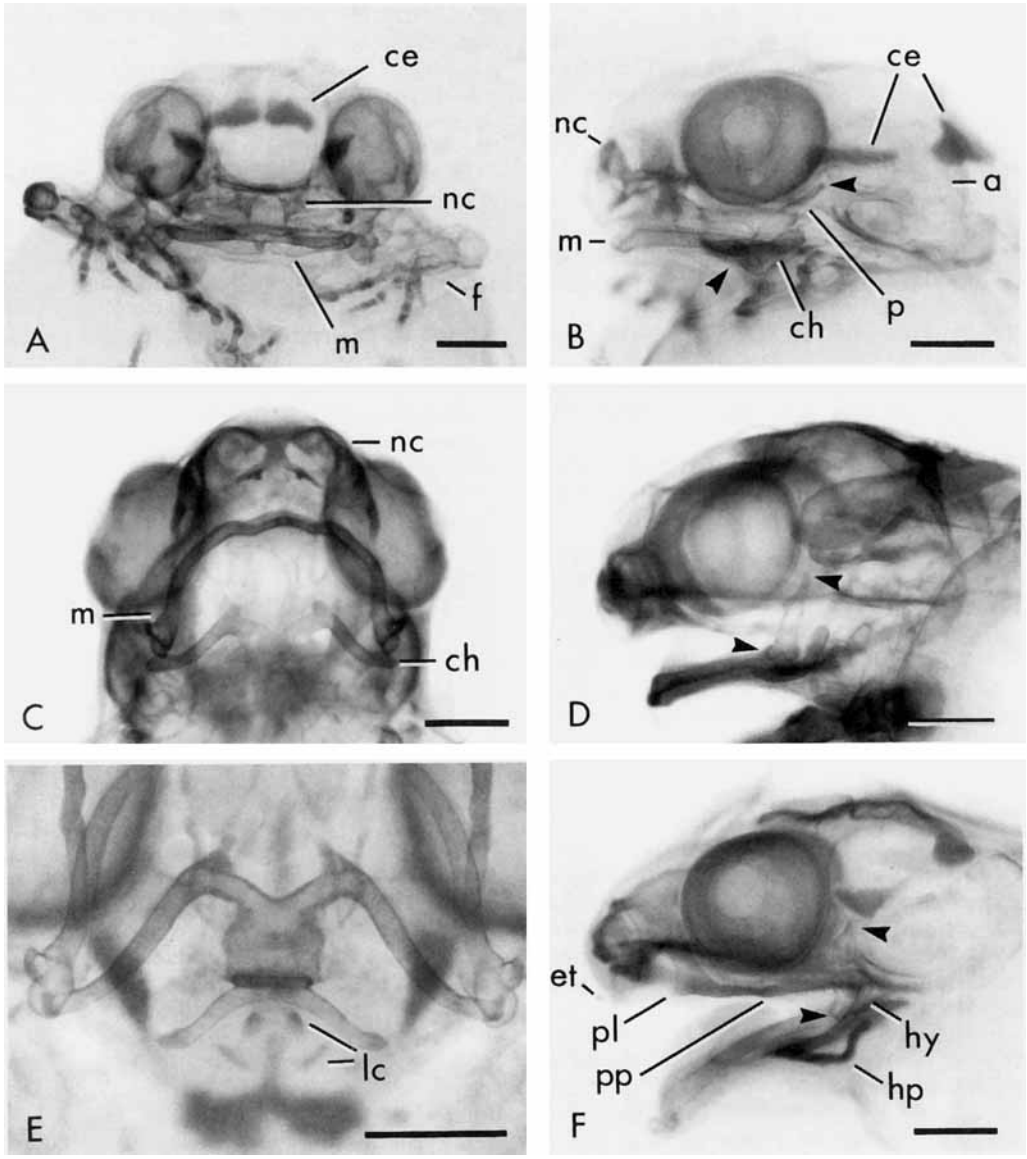

Fig. 4. Immunostained whole-mounts depicting cranial development at T-S Stages 12 (**A,B**), 13 (**C,D**), and 14 (**E,F**). A: Anterior view. B, D, and F: Lateral view. C: Anteroventral view. E: Ventral view of hyobranchial skeleton. Arrowheads as in Figure 2. Additional abbreviations: et, egg tooth; hp, hyoid plate; hy, hyale; lc, laryngeal cartilages; nc, nasal capsule; pl, planum antorbitale. Scale bars = 0.5 mm.

apophyses appear to have fused to form a thin, continuous bridge between adjacent vertebrae. All limb and limb-girdle cartilages are distinct, as before.

The neurocranium is more extensive, especially anteriorly (Fig. 4A,B). Sphenethmoidal cartilages (septum, solum, and tectum nasi, planum antorbitale) are more robust, and a number of additional nasal capsular cartilages (e.g., alary cartilage, oblique cartilage, superior, and inferior prenasal cartilages) are visible in whole-mounts or sections. Nodules of calcified endolymph within the braincase are prominent and symmetrical, but the middle portion of each is very thin. The mandible is more elongate rostrocaudally, correspond-

ing to the ongoing posteriad migration of the jaw articulation; it is beginning to assume the characteristic, adult, inverted U-shape in dorsal view. Anteromedial segments are still sickle-shaped and thinner than adjacent regions, but less so than in earlier stages. The palatoquadrate is stout, especially at the articular process, but tapers somewhat at the otic process; its long axis is oriented at 55°. The otic process is close to the auditory capsule but the two elements remain separated by a small gap.

The hyobranchial skeleton is little changed from Stage 11 (Fig. 6). The ceratohyal articulates with the palatoquadrate midway between articulating and otic processes (Fig. 4B).

A pair of rudimentary egg teeth are visible as tiny keratinized cones at the tip of the snout immediately above the mouth.

Stage 13 (Fig. 4C,D). The notochord no longer stains positive for collagen in the head or trunk; staining in the caudal portion, which is smaller than in the preceding stage, is faint. In the postcranial skeleton, strong staining for collagen is limited to growth zones (e.g., long bone epiphyses, neural arches), except for the distal portions of the limbs, which remain well stained. Staining is much more intense in Alcian-alizarin preparations. Centers of ossification are visible within both the trunk vertebrae (neural arches) and the appendicular skeleton. Opposing neural arches approach one another dorsally; pre- and postzygapophyses and transverse processes are distinct. The latter are especially pronounced opposite the pectoral and pelvic girdles.

The neurocranium is well formed, especially anteriorly, where it closely resembles that of a postmetamorphic frog (Fig. 4C,D). Calcified endolymph within the braincase resembles that seen at Stage 12 (Fig. 4A,B) except that anterior and posterior segments on each side are connected by a threadlike bridge; posterior segments approach or articulate at the dorsal midline at the level of the synotic tectum. Additional deposits are visible for the first time within each auditory capsule. The mandible is more elongate; the jaw articulation lies posterior to the optic foramen. Anteromedial segments (infrarostral cartilages) now occupy a very small portion of the lower jaw; the symphysis is distinctly notched along its ventral margin. The palatoquadrate is nearly vertical (85°); the otic process articulates and is beginning to fuse with the anterolateral face of the auditory capsule. (Prechondrogenic condensations linking these elements are visible in sections.) A rudimentary pseudobasal process is present on the medial aspect of each palatoquadrate between the articulation with the ceratohyal and the otic process.

Hyobranchial anatomy is variable. The skeleton in one specimen (not illustrated) is only slightly modified from that at Stage 12. Ceratohyals are prominent and elongate. Anterior processes are rudimentary, and lateral segments (hyale) still articulate with the palatoquadrate. Ceratobranchial I is arrayed parallel to the hyale, but it is only slightly more than half as long and tapers distally. The threadlike CB II is arrayed transversely and is about half as long as CB I. Similarly, ceratobranchial III is short and thin; CB IV is broader and, including the portion proximal to CB III, is nearly as long as CB I. Another immunostained specimen is more advanced (Figs. 4C,D, 6). In it, a thin cartilaginous bridge extends anterodorsally from each hyale to fuse with the anteroventral margin of the auditory capsule; distal regions of CB I–III have been resorbed and cartilage is filling in the area between the proximal portions of the ceratohyal and CB I to form the hyoid plate.

The pair of cornified egg teeth rudiments is more prominent.

Stage 14 (Fig. 4E,F). The notochord is similar to that at Stage 13, only shorter caudally. Otherwise, collagen-positive areas generally are limited to cartilaginous epiphyses throughout the entire postcranial skeleton. Opposing neural arches closely approach one another or articulate dorsally; vertebral centra are well developed laterally, but are incomplete above and below the notochord. Long bones, especially proximal elements, are ossified for most of their length.

The cartilaginous walls, floor, and roof of the neurocranium are nearly fully formed, anteriorly and posteriorly (Fig. 4F). Prominent deposits of calcified endolymph lie within both the braincase and each auditory capsule, little changed from Stage 13. The mandible also generally resembles that at Stage 13. The short palatoquadrate is oriented at 95°, reflecting the continued posteriad migration of the jaw articulation, which now lies beneath the auditory capsule. The prominent pterygoid process extends anteriorly, subtending the orbit, before fusing with the planum antorbitale of the nasal capsule (= lamina orbitonasalis of earlier embryo); the otic process is fused to the anterolateral face of the

auditory capsule. A small pseudobasal process extends medially from a point just dorsal to the jaw articulation to establish a second contact between the palatoquadrate and the auditory capsule.

The hyolaryngeal skeleton has changed substantially from earlier stages (Figs. 4E, 6). It now comprises an urn-shaped hyoid plate; paired hyale derived from the ceratohyals, each with a prominent anterior process; and paired posteromedial processes, each derived from CB IV plus the basal portion once shared with CB III. Ceratobranchials I, II, and III are absent as discrete elements, although their basal portions, especially that of CB I, have been incorporated into the hyoid plate. The distal, recurved portion of each hyale is fused to the auditory capsule via the short cartilaginous segment described earlier (Stage 13). Rudimentary laryngeal cartilages, variably present at Stage 13, are present posterodorsal to the posteromedial processes of the hyoid plate (Fig. 4E).

Paired egg teeth rudiments have merged to form a single, larger, and more prominent tooth.

Stage 15 (Fig. 5A–D). The postcranial skeleton is well developed. Neural arches are well ossified; paired, basal ossification centers on either side of the notochord correspond to the developing vertebral centra. Ossification centers are visible throughout the appendicular skeleton, including many distal phalanges. Collagen-positive staining is limited to the caudal portion of the notochord, which is continuing to resorb and is about as long as the thigh; to the distal tips of transverse processes; and to the dorsomedial segments of the neural arches.

The cartilaginous skull and hyobranchium generally resemble those of Stage 14, although much of the cartilage is being replaced by bone (Figs. 5A–D, 6). Except for the mandible and the hyobranchial skeleton, which remain collagen-positive, whole-mount immunostaining is less intense than at earlier stages. The adultlike mandible is elongate and sinuous, especially at the symphysis (Fig. 7B). Anterior processes of the hyale are longer (Fig. 6). Calcified endolymph resembles that at Stage 14. The median egg tooth is prominent.

Bony skull

In *Eleutherodactylus coqui,* 13 of the adult complement of 17 cranial bones appear during the embryonic period (Table 2); all are visible in serial sections or alizarin-stained whole-mounts at Stage 15. One additional bone, the vomer, develops within 2 mo posthatching. The most conspicuous feature of the early sequence of bone formation is precocious ossification of bones associated with the jaw. Typically, the first two bones to appear are the angulosplenial and squamosal, which partly invest the lower jaw and jaw suspensorium, respectively. Six of the first eight bones to form contribute to the upper and lower jaws or jaw suspensorium—angulosplenial, squamosal, premaxilla, pterygoid, dentary, and maxilla.

In general, bones are first visible in serial sections one or two stages earlier than in whole-mounts. For example, no bone was visible in whole-mounts earlier than Stage 13, whereas four bones were visible in sections at Stage 12 (Table 2). This is especially true for thin bones that lie deep within the head, e.g., septomaxilla, and which, in early stages of ossification, may be difficult to see in whole-mounts. Brief descriptions of the embryonic or posthatching (vomer) development of each bone are provided below.

Angulosplenial

The angulosplenial is visible in sections beginning at Stage 12 and in all whole-mounts beginning at Stage 13 (Fig. 8A). It forms as a thin bone that runs along the medial (anteriorly) or ventral (posteriorly) margin of Meckel's cartilage. Initially, it extends from an anterior level ventral to the planum antorbitale, posteriorly to the jaw articulation. By Stage 13, it is hollow and either round or triangular in cross section (Fig. 8B), and by Stage 15 it extends rostrally to the medial curvature of Meckel's cartilage (Fig. 5B).

Squamosal

Like the angulosplenial, the squamosal is visible in sections beginning at Stage 12 and in all whole-mounts beginning at Stage 13 (Fig. 8). It first appears as a short posterodorsal rod (otic ramus) or anteroventral splint (ventral ramus) of bone embedded within a condensation of cells investing the palatoquadrate cartilage laterally from the otic process to the jaw articulation (Fig. 8B). At Stage 13, the otic ramus extends posteriorly alongside the auditory capsule (Fig. 8A). By Stage 15, the squamosal is distinctly biarmed, with a short zygomatic ramus anteriorly delimiting otic and ventral rami (Fig. 5D).

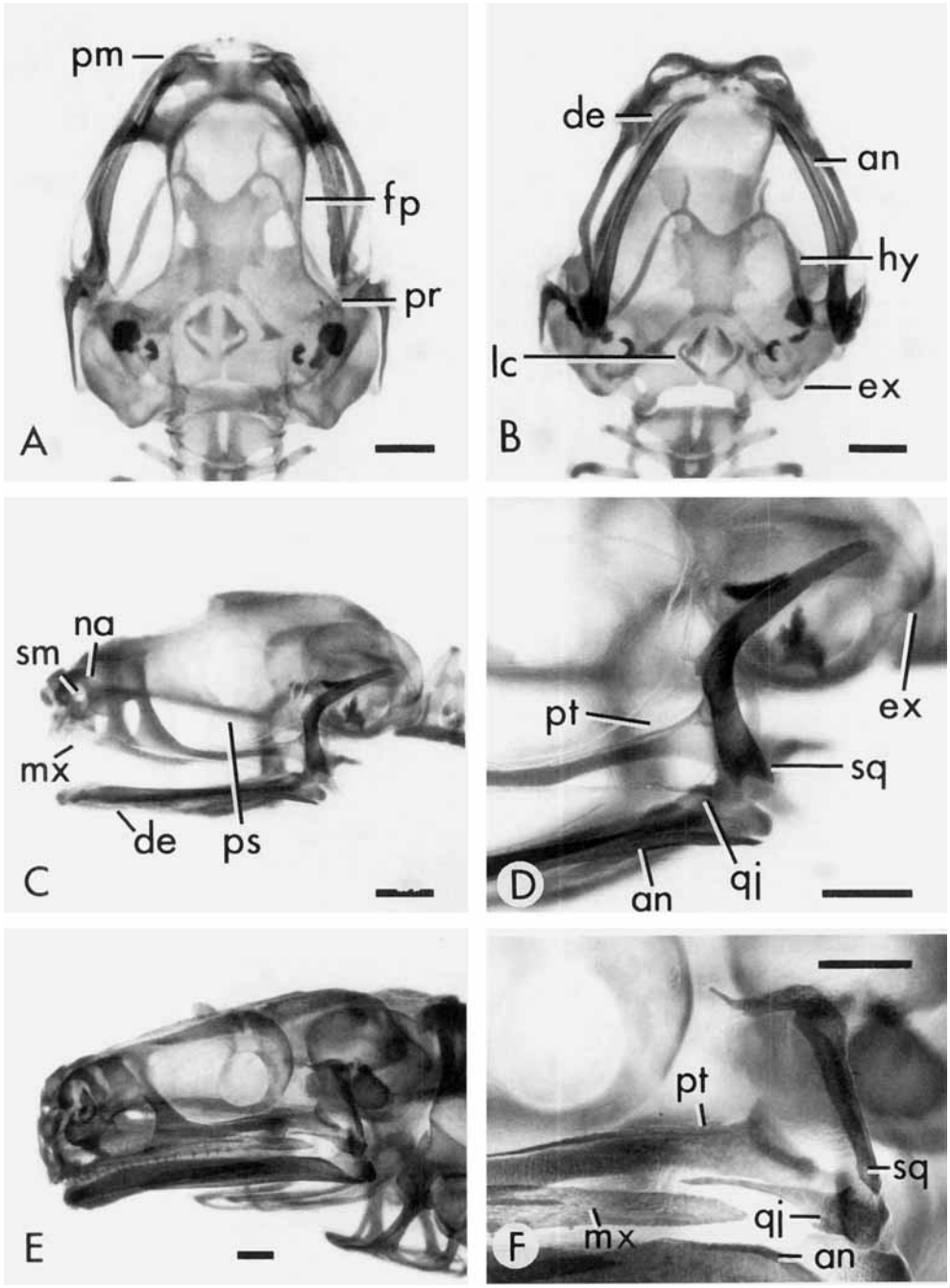

Fig. 5. **A–C:** Alcian/alizarin-stained skull of *Eleutherodactylus coqui* several weeks posthatching (T-S 15+), seen in dorsal, ventral, and lateral views, respectively. **D:** Close-up of the jaw region in C. **E:** Skull of a newly metamorphosed froglet of the Oriental fire-bellied toad, *Bombina orientalis* (lateral view). **F:** Close-up of the jaw region in E. Additional abbreviations: an, angulosplenial; de, dentary; ex, exoccipital; fp, frontoparietal; mx, maxilla; na, nasal; pm, premaxilla; pr, prootic; ps, parasphenoid; pt, pterygoid; qj, quadratojugal; sm, septomaxilla; sq, squamosal. Scale bars = 0.5 mm.

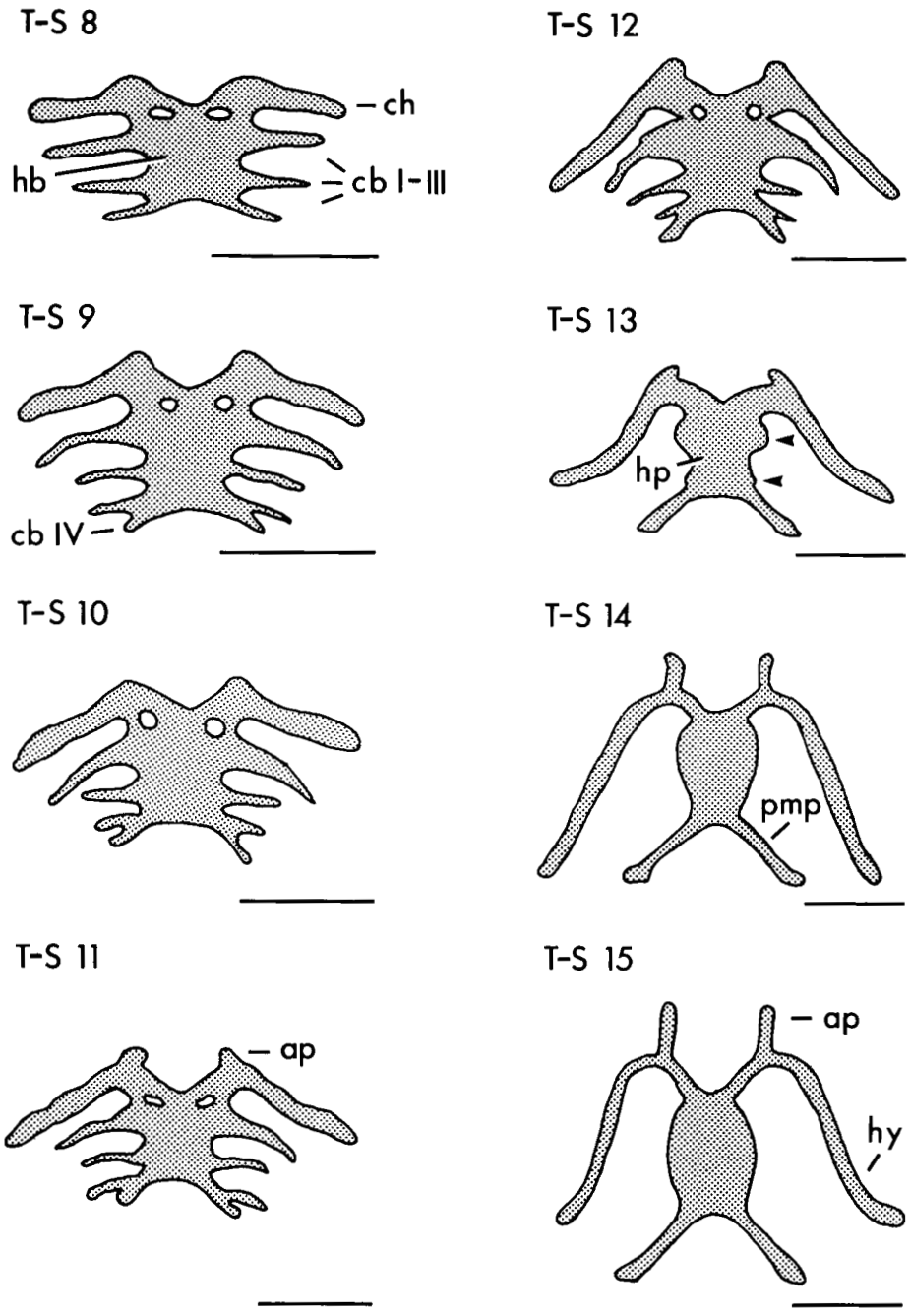

Fig. 6. Ontogeny of the hyobranchial skeleton during embryonic development in *Eleutherodactylus cogui*. Illustrations are drawn from immunostained and Alcian/alizarin-stained whole-mounts; all are ventral views. Arrowheads in T-S 13 indicate traces of ceratobranchials I and II. Additional abbreviations: ap, anterior process; cb, ceratobranchial; hb, hypobranchial plate; pmp, posteromedial process. Scale bars = 0.5 mm.

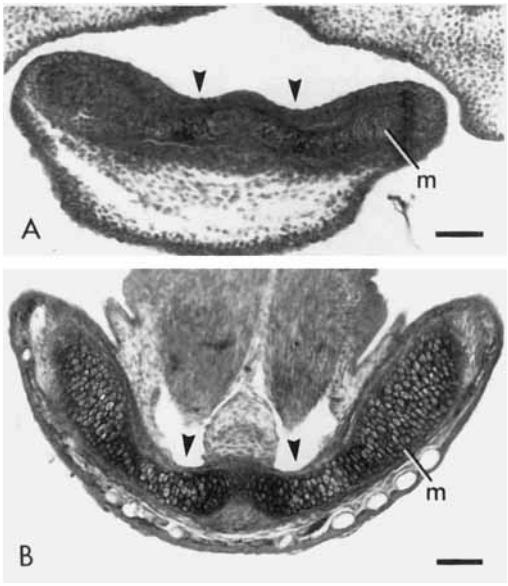

Fig. 7. Transverse sections through the mandibular symphysis of *Eleutherodactylus coqui* at T-S Stages 11 (**A**) and 15 (**B**). Arrowheads denote thinner, anteromedial segments of the mandible (m) that correspond to the infrarostral cartilages and which are continuous with Meckel's cartilage (lateral segments). Scale bars = 0.1 mm.

Parasphenoid

The parasphenoid forms as a thin, narrow sheet of bone that initially invests the ventromedial surface of the neurocranium between the anterior portions of the auditory capsules. Although visible in sections at Stage 12, it is not reliably seen in whole-mounts until Stage 15 (Fig. 5C). By Stage 14, the cultriform process extends rostrally to the level of the optic foramen. By Stage 15, the paired alae extend laterally beneath the auditory capsules, and the cultriform process nearly reaches the level of the planum antorbitale.

TABLE 2. Embryonic and early posthatching ossification sequence in Eleutherodactylus coqui[1]

Townsend–Stewart stage	Bone
12	[Angulosplenial, Squamosal]
	[Parasphenoid, Premaxilla]
13	[Frontoparietal, Pterygoid, Dentary, Maxilla, Exoccipital]
14	[Septomaxilla, Quadratojugal]
15	[Prootic, Nasal]
15+	Vomer

[1]Bones are listed according to the earliest stage that they were observed, either in serial sections or whole-mounts. Ossification sequence among bones contained within each set of brackets could not be determined from the material available. Hatching occurs during Stage 15. The vomer first appears within 2 mo posthatching.

Premaxilla

The premaxilla is a triradiate bone that forms in the tip of the snout anteroventromedial to the olfactory organ. It is first visible in sections at Stage 12, when it has established an articulation with the ventral end of the superior prenasal cartilage of the nasal capsule. Subsequently, the three rami—pars dentalis, alary process, and pars palatina—grow laterally, dorsally, and caudally, respectively. The premaxilla is readily seen in whole-mounts at Stage 15 (rarely 14), when the paired elements approach one another in the midline (Fig. 5A); they lie dorsal to the median egg tooth.

Frontoparietal

The frontoparietal forms as a thin sheet of bone that initially (Stage 13) invests the lateral margin of the neurocranium (taenia tecti marginalis) above the eye. By Stage 14, it comprises a thin, bony splint along the dorsolateral margin of the neurocranium that extends rostrally to the level of the planum antorbitale. By Stage 15, when it is first visible in whole-mounts, it spans virtually the entire orbital region of the neurocranium (Fig. 5A).

Pterygoid

The pterygoid is first visible (Stage 13) as a thin bone medial to the articular process of the palatoquadrate cartilage and immediately anterior to the jaw articulation. Subsequently, it grows rostrally as a thin rod along the dorsal edge of the pterygoid process ventral to the auditory capsule. When first visible in whole-mounts at Stage 15, it is already triradiate (Fig. 5D). The extremely thin, elongate anterior ramus extends toward but does not yet articulate with the maxilla; the much shorter posterior arm articulates laterally with the palatoquadrate and the short medial ramus articulates with the auditory capsule.

Dentary

The dentary is first visible in serial sections at Stage 13 and in whole-mounts at

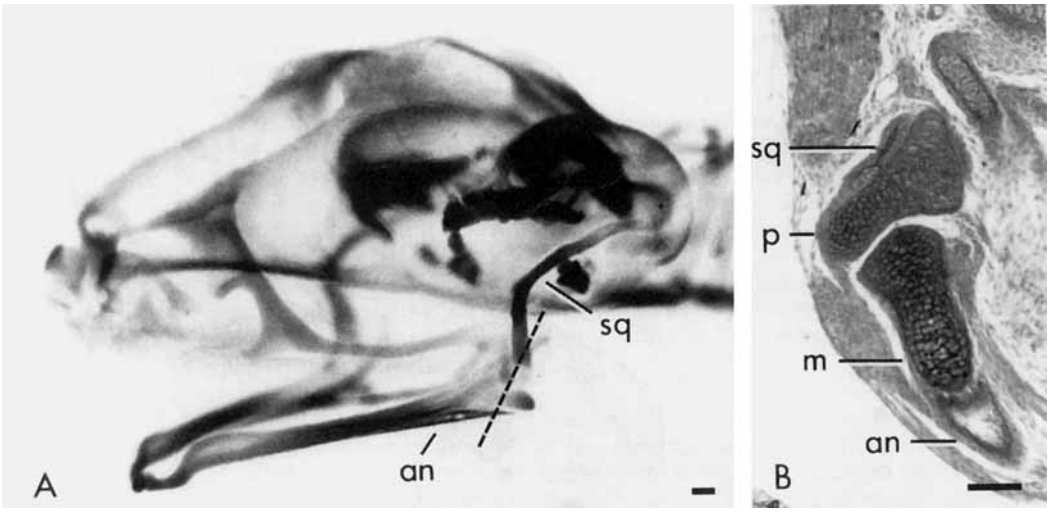

Fig. 8. **A:** Alcian/alizarin-stained skull of *Eleutherodactylus coqui*, T-S Stage 13 (lateral view), showing the first two bones to form—the squamosal (sq) and angulosplenial (an). **B:** Transverse section through the jaw articulation at the same stage, showing the relationship of these bones to the mandible (m) and the palatoquadrate cartilage (p). Dashed line in A denotes the approximate plane of section in B. Scale bars = 0.1 mm.

Stage 14 (rarely 13). Initially, the dentary invests the anterolateral margin of Meckel's cartilage. By Stage 14, it almost completely encircles the paired anteromedial segment of the mandible (infrarostral cartilage); this region, which corresponds to the Mentomeckelian bones of the adult, does not ossify independently of the remainder of the dentary. By hatching (Stage 15), the caudal tip of the dentary lies ventral to the anterior margin of the orbit and broadly overlaps (in lateral view) the angulosplenial, which invests Meckel's cartilage along its medial edge (Fig. 5B,C).

Maxilla

The maxilla initially (Stage 13) invests the posterior maxillary process of the neurocranium ventral to the eye. Along much of its length, it is triradiate in cross section. The long pars dentalis and the much shorter pars palatina sheathe the lateral and medial faces of the posterior maxillary process, respectively; the short pars dentalis descends ventrally. The maxilla subsequently grows both rostrally and caudally. By Stage 14, it extends rostrally beyond the anterior maxillary process to a position ventrolateral to the nasal capsule; posteriorly, it tapers to an extremely thin rod that extends to the level of the auditory capsule. In whole-mounts (Stage 15), it closely approaches but remains separate from the premaxilla anteriorly, and the quadratojugal posteriorly (Fig. 5C).

Exoccipital

The exoccipital is first visible (Stage 13) as a thin layer of bone covering the posterior face of the occipital arch, opposite the neural arch of the adjacent atlas vertebra. By hatching, it has encroached onto the remainder of the occipital arch and replaced this cartilage as well as the adjacent posteromedial portion of the auditory capsule (Fig. 5B,D).

Quadratojugal

The quadratojugal is first visible at Stage 14 along the ventrolateral surface of the articular process of the palatoquadrate, where it articulates with the ventral ramus of the squamosal. At this stage it also extends anteriorly a very short distance as an extremely thin rod lateral to the jaw adductor musculature. The quadratojugal typically is first visible in whole-mounts at Stage 15, and rarely at 14 (Fig. 5D).

Septomaxilla

The septomaxilla is a small bone that forms in the ventrolateral part of the olfactory organ, between the nasolacrimal duct and the lateral edge of the solum nasi, which forms the floor of the nasal capsule (Fig. 5C). It may be present as a tiny speck of bone seen in sections at Stage 13, but it is first clearly visible at Stage 14. By Stage 15, the bone may span as few as five consecutive sections, yet it is easily seen in the majority of whole-

mounts, embedded in nasal capsular cartilage ventral to the external naris.

Prootic

The prootic forms as a center of endochondral ossification within the anteromedial wall of the auditory capsule adjacent to the basal plate (Fig. 5A). It is first visible at Stage 15 in both whole-mounts and serial sections. In all whole-mounts examined, the prootic forms in a region of capsular cartilage that lies between nodules of calcified endolymph within the auditory capsule and the braincase.

Nasal

The nasal initially forms as a thin, nearly transverse sliver of bone that straddles the surface of the nasal capsule, posterior to the oblique cartilage and dorsal to the planum terminale (Fig. 5C). Its presence is presaged by a distinct condensation of cells seen in serial section at Stage 14, but calcified matrix is not present until Stage 15, when, typically, the bone also is visible in whole-mounts.

Vomer

The vomer is a paired bone that is first visible in whole-mounts preserved within 2 mo after hatching; it is absent from all prehatching specimens, both whole-mounts and serial sections. It initially forms ventral to the braincase, anteromedial to the orbit. It comprises an extremely thin, longitudinal process that extends rostrally toward the internal naris and which is continuous caudally with a short, transverse dentigerous process. The structure of the vomer was not examined in sections.

DISCUSSION

Recapitulation vs. repatterning

A recurring question in the study of direct-developing anurans is whether there is an embryonic recapitulation of the ancestral biphasic pattern of development—including an embryonic "metamorphosis"—or if, instead, there has been a more fundamental repatterning of early ontogeny. Such repatterning may involve the loss of ancestral, larval structures, shifts in the relative timing of developmental events (i.e., heterochrony), and, perhaps most significantly, the appearance of novel morphologies not present in the ancestor. From the limited comparative data available, the degree of recapitulation vs. repatterning varies widely, as one might expect from lineages that have evolved direct development independently (reviewed by Lutz, '47, '48; Lynn, '61; Orton, '51). *Eleutherodactylus* is generally regarded as the least recapitulatory of all direct-developing anurans (Elinson, '90; Hughes, '65, '66; Lynn, '61; Orton, '51), although some authors refer to a metamorphosis during embryonic development (Adamson et al., '60; Infantino et al., '88). Much of the difficulty in resolving this question stems from the difficulty in visualizing the morphology of early embryonic structures, which typically are small, transient, and not fully differentiated. This problem is especially acute for the development of internal features such as the skeleton, for which subtle aspects of form are difficult or time-consuming to depict by using traditional histological methods, either in whole-mounts or serial sections.

In this study, we employed a new whole-mount immunohistochemical technique that offers greater resolving power for depicting the structure of developing tissues with virtually no preparation artifact (Dent et al., '89; Dent and Klymkowsky, '89; Klymkowsky and Hanken, '91). For cartilages, it reveals the form of developing elements from the time of initial deposition of the extracellular matrix component Type II collagen at the inception of their development. This allowed us to depict the earliest stages of cranial chondrogenesis and, thereby, address more completely the question of recapitulation vs. repatterning as it applies to the skull. Both phenomena were observed.

The most conspicuous evidence of repatterning of cranial ontogeny in *Eleutherodactylus coqui* is the absence of a number of exclusively larval cartilages found in metamorphosing anurans. These include the suprarostral cartilages, which constitute the tadpole's upper jaw; the commissura quadratocranialis anterior (de Beer, '37), which unites the palatoquadrate with the neurocranium anteriorly; the cornua trabeculae, paired anterolateral extensions of the braincase; and muscular, larval otic, and ascending processes of the palatoquadrate. In the absence of these cartilages, the development of other cartilages that follow or replace them at metamorphosis has been advanced into earlier stages. For example, the postmetamorphic complex of nasal cartilages (e.g., solum nasi, septum nasi, planum antorbitale) begins to form as early as Stage 9, only two stages after cartilage is first visible anywhere in the head.

Evolutionary modifications to the ontogeny of other cranial cartilages are more complicated. While lacking the earliest, or larval characteristics of metamorphosing taxa, these structures do not initially display their final adult, or postmetamorphic, configuration. Instead, they first assume a "mid-metamorphic" stage of development that is subsequently remodeled before hatching. In short, there is both repatterning and partial recapitulation of the ancestral ontogeny. The two principal examples of this phenomenon are components of the visceral skeleton: the lower jaw and jaw suspensorium, and the hyobranchial skeleton.

In most metamorphosing frogs, the larval palatoquadrate is a massive cartilage that extends anteroventrally from the level of the auditory capsule to a position ventral to the snout where it articulates with the short, transverse Meckel's cartilage. The latter, in turn, articulates medially with the infrarostral cartilage, and together these paired cartilages constitute the tadpole's lower jaw. At metamorphosis, the palatoquadrate undergoes a profound transformation during which it shortens, reorients to a nearly vertical position, and establishes a solid connection with the auditory capsule. Meckel's and infrarostral cartilages correspondingly fuse, and the resulting mandible elongates as the jaw joint migrates caudally to a position ventrolateral to the otic region (Hanken and Summers, '88a; de Jongh, '68; Sedra, '50; Wassersug and Hoff, '82; Fig. 9).

In *Eleutherodactylus coqui,* three exclusively larval characteristics of the palatoquadrate—muscular, larval otic, and ascending processes—never form. (Otic and pterygoid processes, which are both found in larval frogs and retained after metamorphosis, are present very early.) However, with respect to its elongate form, anteroventral orientation, and the location of the jaw joint rostral to the auditory capsule, the palatoquadrate initially (Stage 8) and in several subsequent stages resembles a biphasic anuran in mid-metamorphosis. It eventually shortens and reorients to a nearly vertical position, and only shortly before hatching (Stages 14, 15) establishes solid connections with the auditory capsule via the otic and pseudobasal processes. Paralleling these changes in the palatoquadrate, Meckel's cartilage forms initially as a short, transverse, subrostral cartilage that subsequently assumes the elongate, inverted-U configuration characteristic of postmetamorphic stages. Finally, while paired infrarostral cartilages, separate from and articulating with Meckel's cartilages laterally, never form, anteromedial segments of the mandible that are crescentic and thinner than laterally adjacent portions are visible beginning at Stage 10 (Figs. 3C,E, 7). These segments resemble infrarostral cartilages of biphasic anurans during mid-metamorphosis, when they are fusing to Meckel's. Thus, while discrete infrarostral cartilages are not present in *E. coqui,* segments of the mandible corresponding to them, and already fused to Meckel's cartilage, can be readily identified.

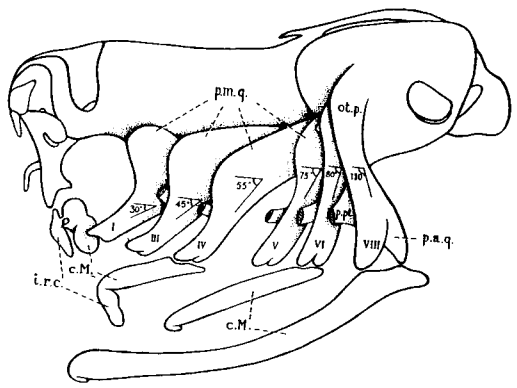

Fig. 9. Sedra's ('50) composite representation of the progressive posteriad displacement of the jaw suspensorium during anuran metamorphosis, seen here in *Rana.* The shape and position of the palatoquadrate (p.a.q.) are depicted in sequential stages (roman numerals); arabic numerals indicate the corresponding angle between the palatoquadrate and the skull base. Morphology of the left lower jaw (c.M., Meckel's cartilage; and i.r.c., infrarostral cartilage) is depicted for four stages. Most of the pterygoid process (p.pt.) has been cut away. Additional abbreviations: ot.p., otic process; p.m.q., muscular process of the quadrate. Reproduced *with permission* from Sedra ('50).

A similar embryonic transformation takes place in the developing hyobranchial skeleton, but the changes observed are even more dramatic than those seen in the lower jaw and jaw suspensorium (Fig. 6). When the cartilaginous hyobranchial skeleton initially forms at Stage 8, there is an obvious segmental pattern involving the anterior ceratohyal and posterior ceratobranchials I–III; ceratobranchial IV appears at Stage 9. While this arrangement generally resembles that seen in the hyobranchial skeleton of larval anurans, there are at least two important differences. First, in *E. coqui,* the various component elements do not articulate with

one another, but instead form a single continuous mass of cartilage; second, the ceratobranchials lack secondary and tertiary branching and are not united distally. Both of these features are characteristic of the hyobranchial skeleton during, but not before, metamorphosis. By Stage 9, however, this configuration begins to be remodeled. Principal changes are reorientation of the ceratohyal, coincident with the posteriad migration of its articulation with the palatoquadrate, and growth and elaboration of the single, median hypobranchial plate. Consequently, by Stage 10, the morphology of the hyobranchial skeleton is substantially different from its initial appearance, and reminiscent of a mid-metamorphic stage in biphasic anurans.

A second period of intense change occurs between Stages 12 and 14. The hyale (formerly ceratohyal) fuses to the auditory capsule and develops an anterior process. An urn-shaped hyoid plate forms that incorporates the hypobranchial plate, basal portions of ceratobranchials I–III, as well as new cartilage. Ceratobranchials I–III are resorbed distally and laryngeal cartilages begin to form. As a result of these modifications, at hatching, the hyobranchial skeleton generally has assumed the "postmetamorphic" configuration of the adult (Fig. 5B).

Some but not all of these exceptional features of cranial development in *Eleutherodactylus* were described in earlier studies. Absence of the suprarostral cartilage and the commissura quadratocranialis anterior was noted in *E. quentheri* (Lynn and Lutz, '46) and *E. nubicola* (Lynn, '42). Lynn ('42) interpreted as cornua trabeculae a pair of small anteromedial cartilages that contribute to the floor of the nasal capsule in *E. nubicola* (Fig. 10, 10 and 7 days before hatching). After studying Lynn's description, however, and comparing it to our own material for *E.*

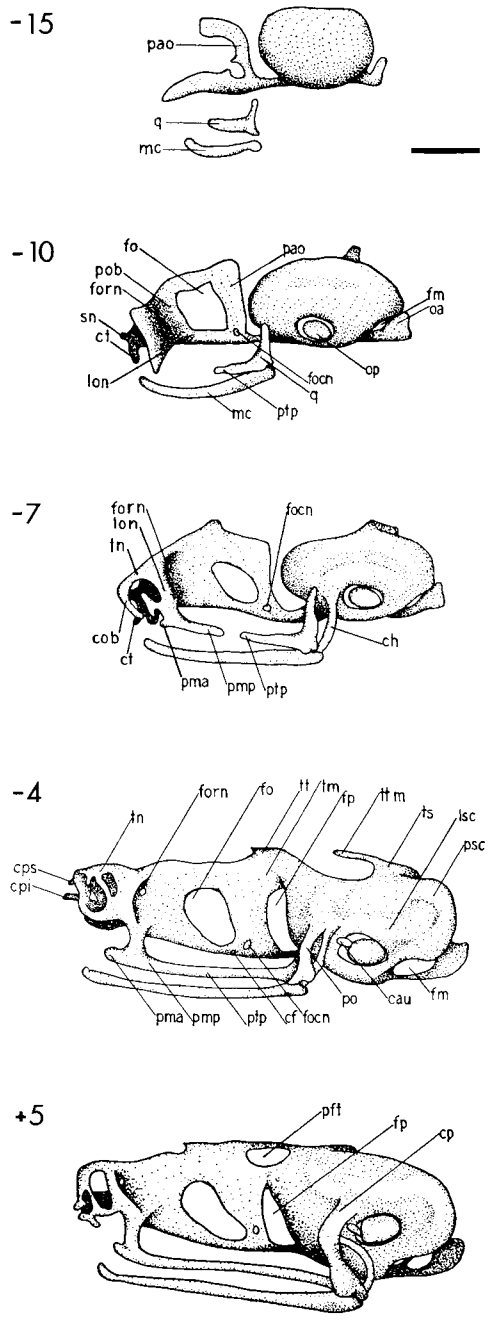

Figure 10

Fig. 10. Lynn's ('42) wax-plate reconstructions of cranial development in *Eleutherodactylus nubicola*. All are lateral views; anterior is to the left. Numbers denote developmental stage (days before [−] or after [+] hatching). Abbreviations: cau, columella auris; cf, carotid foramen; ch, ceratohyal cartilage; cob, cartilage obliqua nasi; cp, crista parotica; cpi, inferior prenasal cartilage; cps, superior prenasal cartilage; ct, cornua trabeculae; fm, fissura metotica; fo, optic foramen; focn, oculomotor foramen; forn, orbitonasal foramen; fp, prootic foramen; lon, lamina orbitonasalis; lsc, lateral semicircular canal; mc, Meckel's cartilage; oa, occipital arch; op, operculum; pao, pila antotica; pft, parietal fontanelle; pma, anterior maxillary process; pmp, posterior maxillary process; po, otic process; pob, preoptic root of orbital cartilage; psc, posterior semicircular canal; ptp, pterygoid process; q, quadrate cartilage; sn, nasal septum; tm, taenia marginalis; tn, tectum nasi; ts, tectum synoticum; tt, tectum transversum; ttm, taenia tecti medialis. Redrawn *with permission* from Lynn ('42). Scale bar = 0.5 mm.'

coqui, we regard these cartilages as distinct from the cornua trabeculae, which, when present, typically extend far anterior from the eventual location of the nasal capsule. Thus, we regard the cornua trabeculae as absent in *E. nubicola,* as well as in *E. coqui.* Absence of muscular, larval otic, and ascending processes of the palatoquadrate has never been reported previously, although it is implicit in Lynn's account of *E. nubicola,* which makes no mention of any of these features either in the text or figures.

The greatest difference between our account of cartilaginous development in *E. coqui* and those available for other species concerns the early development and initial patterning of the lower jaw and jaw suspensorium. Lynn ('42), working from wax-plate reconstructions from serial sections, accurately rendered a number of features involved in the embryonic remodeling of the palatoquadrate and lower jaw in *E. nubicola* (Fig. 10). These include the posteriad migration of the jaw articulation, anteroposterior elongation of Meckel's cartilage, fusion of the pterygoid process to the neurocranium, and fusion of the otic process to the auditory capsule. However, as our results with *E. coqui* show, by the earliest developmental stage that he was able to depict using the methods then available (15 days before hatching, or approximately T-S 9), the morphology of the palatoquadrate and Meckel's cartilage is already different from the initial form. For example, the palatoquadrate is depicted by Lynn as initially a triradiate cartilage (Fig. 10), whereas we have shown that this stage is preceded by one in which the palatoquadrate is a straight rod displaced anteroventrally from near the auditory capsule (Fig. 2F). Similarly, while Lynn depicts the jaw articulation initially at the level of the anterior margin of the auditory capsule, associated with a relatively short but longitudinal Meckel's cartilage, in earlier stages the jaw articulation lies even further forward and Meckel's cartilage is shorter and oriented more transversely. In both cases, the earlier stage represents a more larval-like configuration. Finally, infrarostral cartilages are regarded as absent in both *E. nubicola* (Lynn, '42) and *E. quentheri* (Lynn and Lutz, '46). However, neither study provides a detailed description of mandibular morphology that could be used to evaluate if these cartilages are instead incorporated into its anterior portions, as we claim for *E. coqui.*

Lynn's reconstruction of the developing hyobranchial skeleton in *E. nubicola* (Fig. 11) is similar in many respects to that which we observe in *E. coqui* (Fig. 6), although there are at least two significant differences. First, ceratobranchial IV, which has a transient existence in *E. coqui,* "seems to be unrepresented" in *E. nubicola* ('42: p. 51). Second, Lynn's illustration implies that the anterolateral and posterolateral processes that emerge from the hyoid plate in the adult hyobranchial skeleton (Fig. 11F) are homologous with the first two embryonic ceratobranchials (Fig. 11A–E). Yet, in *E. coqui,* ceratobranchials I and II are either completely resorbed or incorporated into the basal plate well before hatching (Figs. 4E, 6), whereas anterolateral and posterolateral processes form de novo from the hyoid plate in the weeks after hatching (Fig. 5B); they do not incorporate existing portions of the embryonic ceratobranchials. While it is possible that these two congeneric species differ with respect to these features of hyobranchial skel-

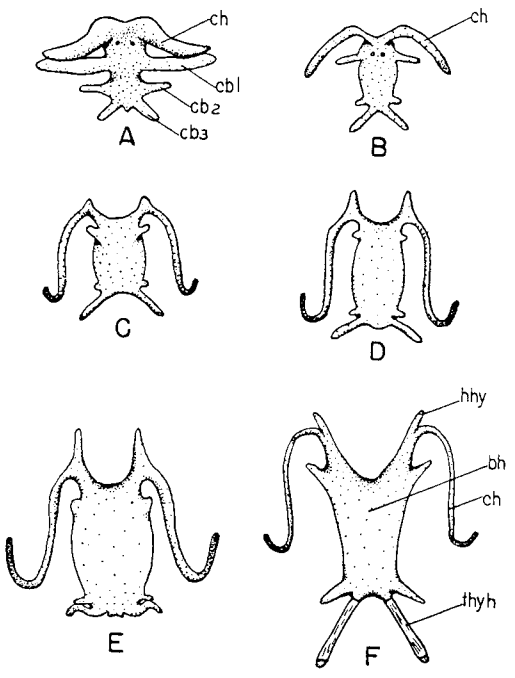

Fig. 11. Lynn's ('42) wax-plate reconstruction of hyobranchial skeletal ontogeny in *Eleutherodactylus nubicola.* Developmental stage (days before [−] or after [+] hatching): **A,** −15; **B,** −10; **C,** −7; **D,** −4; **E,** +5; **F,** adult. Abbreviations: bh, basihyal; cb 1–3, ceratobranchial 1–3; ch, ceratohyal; hhy, hypohyal; and thyh, thyrohyal cartilages. Reproduced *with permission* from Lynn ('42).

etal development, we regard it as equally if not more probable that critical, albeit subtle, details may have been missed by Lynn, who depicted only five embryonic stages of hyobranchial development.

By drawing attention to differences between Lynn's work and ours, we do not mean to deprecate in any way his accomplishments, which represent outstanding contributions to the study of direct development in amphibians. Rather, we offer these comparisons to illustrate the additional resolving power provided by whole-mount immunohistochemistry, as compared to traditional methods for visualizing embryonic form and morphogenesis, and to underscore how critical these early patterning events are for distinguishing recapitulation and repatterning in the ontogeny and evolution of direct development.

Cranial ossification

Cranial ossification in *Eleutherodactylus coqui* differs from that in metamorphosing anurans in two general ways, one of which—the ossification sequence—provides another example of repatterning. First, ossification is initiated during embryogenesis. Indeed, 13 of the adult complement of 17 bones form before hatching, and one more forms within the next 2 mo, when the embryonic yolk supply is exhausted and the hatchling begins to feed. This is very different from metamorphosing anurans, in which ossification typically commences at metamorphosis. In *Bombina orientalis,* for example, osteogenic differentiation is first visible at Gosner ('60) Stage 31, several weeks after the tadpole has begun to feed (Hanken and Hall, '88a). Consequently, the osteocranium of hatchling *E. coqui* bears a striking resemblance to that of a newly metamorphosed froglet (cf. Fig. 5C–F). Thus, in the evolution of direct development in *E. coqui,* bone formation has been advanced into the embryonic period. It is unknown whether those mechanisms that mediate ossification in metamorphosing taxa, such as endocrine factors (Hanken and Hall, '88b), have been retained, or if new mechanisms of control have been developed.

The second general difference concerns the cranial ossification sequence. Notwithstanding significant variation in the order of appearance of later-forming bones, metamorphosing anurans show a remarkably consistent pattern of early ossification. The first bones to form typically are the exoccipital, frontoparietal, and parasphenoid, three bones that invest or reinforce the braincase and otic region (Trueb, '85; de Sá, '88; Wiens, '89). The sequence in *E. coqui* is very different, and primarily involves precocious ossification of the jaws and jaw suspension (Table 2). While the parasphenoid is among the first bones to form, it is preceded by the angulosplenial and the squamosal, two bones which contribute to the jaw suspension and articulation. By the time the exoccipital and frontoparietal have formed, four additional bones are also present: the premaxilla, maxilla, and dentary, three tooth-bearing bones of the upper and lower jaws, and the pterygoid, which braces the jaw suspension against the upper jaw and neurocranium.

The general pattern of ossification in *E. coqui* is consistent with the limited data on bone formation in three other species of *Eleutherodactylus—guentheri* (Lynn and Lutz, '46), *nubicola* (Lynn, '42), and *ricordii* (Hughes, '59). In each species, jaw elements are the first to ossify, which may represent a general and derived feature of skull development in the genus. However, whereas the sequence of ossification apparently is similar among species, the relative timing of bone differentiation is more variable. In *E. nubicola,* for example, formation of the septomaxilla, prootic, and nasal occurs after hatching, whereas these bones form during embryonic development in *E. coqui.* There are no data with which to assess if there are comparable interspecific differences in ossification once feeding begins.

Precocious ossification of jaw elements in direct-developing *Eleutherodactylus* is remarkably similar to the pattern of ossification in the viviparous caecilian *Dermophis mexicanus* (Wake and Hanken, '82). In this species, precocious ossification of the lower jaw and jaw suspension is part of a suite of derived developmental features that represent an embryonic and fetal adaptation that permits intraoviductal feeding by the developing offspring. The derived pattern of ossification in *Eleutherodactylus* may represent a similar trophic adaptation; the jaw elements serve as attachment sites for the prominent adductor and abductor musculature and provide articulations that are important in active feeding, which commences soon after hatching.

Paradox of Eleutherodactylus

In amphibians, the evolution of direct development may have profound morphological, physiological, and ecological consequences

for the lineage involved (Bradford, '84; Bradford and Seymour, '88; Duellman, '89; McDiarmid, '78; Wake, '89). In plethodontid salamanders, fundamental modifications to early ontogeny in some direct-developing taxa are believed to underlie the appearance of major structural innovations in adult morphology, which are absent in related metamorphosing forms (Roth and Wake, '85, '89; Wake, '82; Wake and Roth, '89). According to this model, the evolution of adult structures in metamorphosing taxa is constrained by the presence of larval components which precede them in ontogeny. When, in the evolution of direct development and consequent abandonment of the free-living larval stage, the necessity to form the larval components is removed, this creates the opportunity for evolutionary loss of the larval components and the associated constraint on adult morphology. The principal evidence supporting this model of "ontogenetic repatterning" (Wake and Roth, '89) is the correlation between direct development and morphological novelty, primarily involving the hyobranchial apparatus (Lombard and Wake, '86) and its neural control (Wake et al., '88). There are, however, few embryological data with which to evaluate directly the degree to which the ancestral biphasic ontogeny is actually modified in direct-developing taxa (e.g., Alberch, '87, '89).

Eleutherodactylus offers an excellent opportunity to test the larval constraint hypothesis developed from plethodontid salamanders. Indeed, it is tempting to speculate that the deletion of many larval features during the evolution of direct development in the lineage leading to *Eleutherodactylus* is directly linked to the evolutionary success of the genus, as measured by species diversity. With approximately 450 described species (Hedges, '89), *Eleutherodactylus* is the largest genus of extant terrestrial vertebrates. Yet, in *Eleutherodactylus,* the dramatic modifications to the ancestral ontogeny have had little effect on adult cranial morphology, the variation of which among species is modest for such a large group and which does not differ in any profound way from that of closely related, metamorphosing taxa (Lynch, '71; Wake and Roth, '89). In other words, in *Eleutherodactylus,* the critical factor that could link the observed ontogenetic changes to evolutionary success—morphological novelty and diversification—is lacking. Thus, ontogenetic repatterning is not correlated with extensive morphological diversification and does not seem to be causally linked to the evolutionary success of the genus. If, as seems reasonable, the evolution of direct development is an important causal component in the success of *Eleutherodactylus,* then it may be through associated ecological and/or physiological effects, such as emancipation from aquatic breeding sites and the invasion and occupation of novel terrestrial habitats (Hedges, '89; Heyer, '75). Interestingly, in lacking substantial diversification of adult morphology despite significant ontogenetic change, direct development in eleutherodactyline frogs is remarkably similar to that seen in many echinoderms (Raff, '87; Strathmann, '88).

The developmental basis of direct development

Cranial ontogeny in *Eleutherodactylus* differs substantially from that typical of metamorphosing anurans; it comprises a complex mosaic of ancestral and derived features. The development of many exclusively larval cartilages is omitted entirely, whereas the development of postmetamorphic cartilages and bones, many of which display an ontogenetic sequence unlike the presumed ancestral pattern, is advanced into the embryonic period. These features provide specific examples of repatterning of the ancestral ontogeny. Other components recapitulate in part their metamorphic transformation in metamorphosing species. Yet, the derived pattern of development has had little impact on adult morphology. Clearly, the evolution of direct development in *Eleutherodactylus* involves substantially more than just acceleration and condensation of the ancestral biphasic ontogeny found in metamorphosing anurans. It is thus inappropriate and misleading to describe development in this group as involving a "metamorphosis . . . within the egg" (Adamson et al., '60, p. 467; see also Infantino et al., '88).

Many of the differences in cranial ontogeny between direct-developing *Eleutherodactylus* and metamorphosing frogs may be described effectively in terms of changes in the relative timing and sequence of development, i.e., heterochrony (Elinson, '90). For example, the absence of larval cartilages and corresponding precocious appearance of postmetamorphic structures during embryogenesis in *E. coqui* represents an excellent example of Haeckelian condensation (sensu Gould, '77). Yet, these heterochronic changes likely are only the most obvious manifestation of

fundamental alterations to underlying developmental mechanisms of pattern formation and morphogenesis (Raff and Wray, '89). For example, while it is correct to say that in *Eleutherodactylus* formation of the cornua trabeculae and suprarostral cartilages has been deleted from the ancestral ontogeny, this also means that patterning of the adult neurocranium involves a precursor arrangement that is significantly different from that in metamorphosing frogs. Explanation of derived ontogenetic patterns in terms of specific perturbations of these basic developmental mechanisms poses a compelling challenge to future research on direct development.

A precondition for the evolution of direct development in taxa with complex life cycles may be the independence of larval and adult developmental programs, which allows them to be readily dissociated (Elinson, '90; Raff, '87). Evidence in support of this hypothesis is available for sea urchins (Parks et al., '88; Raff, '87; Wray and McClay, '89; Wray and Raff, '89), but there are fewer data available for amphibians. Degeneration of a number of larval structures at metamorphosis suggests that, in anurans, there is a subset of cell lines that have an exclusively larval fate. Similarly, metamorphosing anurans show early developmental compartmentalization of cell lineages contributing to adult cranial musculature (Alley, '89, '90). Compartmentalization of developmental precursors of larval vs. adult hyobranchial cartilages occurs in the plethodontid salamander *Eurycea bislineata* (Alberch and Gale, '86; Alberch et al., '85) and possibly other plethodontids, but it is not found in primitive urodeles (Alberch, '89). It is not known if compartmentalization of adult components is characteristic of skull development in other amphibians, or even if it applies to features other than the hyobranchial skeleton in plethodontid salamanders. Finally, the fact that many larval cranial components are retained yet significantly remodeled at metamorphosis suggests that there is a third class of cell lineages that have both larval and adult fates. This would seem to be supported by *Eleutherodactylus coqui,* in which several cartilages, instead of completely eliminating the larval developmental program, initially assume an intermediate, mid-metamorphic configuration.

ACKNOWLEDGMENTS

This research was supported by NSF DCB-9019624, NIH 1 R23 DE07190 and 1 F33 DE05610, NIH-BRSG RR07013-20 and RR07013-21, and the Council on Research and Creative Work, CU Boulder (J.H.); by the Pew Biomedical Scholars Award and NSF DCB-890522 (M.W.K.); and by the Hughes Foundation (N.I.). Dr. Thomas Linsenmayer, Tufts University, generously provided his monoclonal antibody to Type II collagen. Drs. Margaret Stewart and Daniel Townsend provided assistance and advice in our attempts to establish a breeding colony of *Eleutherodactylus coqui.* Frogs were collected with the assistance and permission (permits DRN-88-02 and DRN-90-24) of the Puerto Rican Department of Natural Resources and Sr. Eduardo L. Cardona and Sr. Jorge Moreno. Richard Elinson, David Jennings, David Wake, and several anonymous reviewers provided valuable comments on earlier drafts.

LITERATURE CITED

Adamson, L., R.G. Harrison, and I. Bayley (1960) The development of the whistling frog *Eleutherodactylus martinicensis* of Barbados. Proc. Zool. Soc. Lond. *133:* 453–469.

Alberch, P. (1987) Evolution of a developmental process—irreversibility and redundancy in amphibian metamorphosis. In R.A. Raff and E.C. Raff (eds): Development as an Evolutionary Process. New York: Alan R. Liss, Inc., pp. 23–46.

Alberch, P. (1989) Development and the evolution of amphibian metamorphosis. In H. Splechtna and H. Hilgers (eds): Trends in Vertebrate Morphology, Fortschritte der Zoologie, Vol. 35. Stuttgart: Gustav Fischer Verlag, pp. 163–173.

Alberch, P., and E.A. Gale (1986) Pathways of cytodifferentiation during the metamorphosis of the epibranchial cartilage in the salamander *Eurycea bislineata.* Dev. Biol. *117:*233–244.

Alberch, P., G.A. Lewbart, and E.A. Gale (1985) The fate of larval chondrocytes during the metamorphosis of the epibranchial in the salamander *Eurycea bislineata.* J. Embryol. Exp. Morphol. *88:*71–83.

Alley, K.E. (1989) Myofiber turnover is used to retrofit frog jaw muscles during metamorphosis. Am. J. Anat. *184:*1–12.

Alley, K.E. (1990) Retrofitting larval neuromuscular circuits in the metamorphosing frog. J. Neurobiol. *21:* 1092–1107.

Altig, R., and G.F. Johnston (1989) Guilds of anuran larvae: relationships among developmental modes, morphologies, and habitats. Herp. Monogr. *3:*81–109.

Bradford, D.F. (1984) Physiological features of embryonic development in terrestrially-breeding plethodontid salamanders. In R.S. Seymour (ed): Respiration and Metabolism of Embryonic Vertebrates. Dordrecht: Dr. W. Junk Publ., pp. 87–98.

Bradford, D.F., and R.S. Seymour (1988) Influence of environmental PO_2 on embryonic hatching oxygen consumption, rate of development, and hatching in the frog *Pseudophryne bibroni.* Physiol. Zool. *61:*475–482.

de Beer, G.R. (1937) The Development of the Vertebrate Skull. Oxford: Oxford University Press. (Paperback reprint: University of Chicago Press, Chicago, 1985.)

de Jongh, H.J. (1968) Functional morphology of the jaw apparatus of larvae and metamorphosing *Rana temporaria* L. Neth. J. Zool. *18:*1–103.

Dent, J.A., and M.W. Klymkowsky (1989) Whole-mount analyses of cytoskeletal organization and function during oogenesis and early embryogenesis in *Xenopus*. In H. Shatten and G. Shatten (eds): The Cell Biology of Fertilization. Monographs in Cell Biology. New York: Academic Press, pp. 63–103.

Dent, J.A., A.G. Polson, and M.W. Klymkowsky (1989) A whole-mount immunocytochemical analysis of the expression of the intermediate filament protein vimentin in *Xenopus*. Development *105:*61–74.

de Sá, R.O. (1988) Chondrocranium and ossification sequence of *Hyla lanciformis*. J. Morphol. *195:*345–355.

Dingerkus, G., and L.D. Uhler (1977) Enzyme clearing of alcian blue stained whole small vertebrates for demonstration of cartilage. Stain Technol. *52:*229–232.

Duellman, W.E. (1989) Alternative life-history styles in anuran amphibians: evolutionary and ecological implications. In M.N. Bruton (ed): Alternative Life-History Styles of Animals. Dordrecht: Kluwer Academic Publ., pp. 101–126.

Duellman, W.E., and L. Trueb (1986) Biology of the Amphibians. New York: McGraw-Hill Co.

Elinson, R.P. (1990) Direct development in frogs: wiping the recapitulationist slate clean. Semin. Dev. Biol. *1:*263–270.

Elinson, R.P., E.M. del Pino, D.S. Townsend, F.C. Cuesta, and P. Eichhorn (1990) A practical guide to the developmental biology of terrestrial-breeding frogs. Biol. Bull. *179:*163–177.

Gosner, K.L. (1960) A simplified table for staging anuran embryos and larvae with notes on identification. Herpetologica *16:*183–190.

Gould, S.J. (1977) Ontogeny and Phylogeny. Cambridge: Harvard Univ. Press.

Hall, B.K. (1985) The role of movement and tissue interactions in the development and growth of bone and secondary cartilage in the clavicle of the embryonic chick. J. Embryol. Exp. Morphol. *93:*133–152.

Hanken, J. (1989) Development and evolution in amphibians. Am. Sci. *77:*336–343.

Hanken, J., and B.K. Hall (1988a) Skull development during anuran metamorphosis: I. Early development of the first three bones to form—the exoccipital, the parasphenoid, and the frontoparietal. J. Morphol. *195:* 247–256.

Hanken, J., and B.K. Hall (1988b) Skull development during anuran metamorphosis: II. Role of thyroid hormone in osteogenesis. Anat. Embryol. (Berl.) *178:*219–227.

Hanken, J., and C.H. Summers (1988a) Skull development during anuran metamorphosis: III. Role of thyroid hormone in chondrogenesis. J. Exp. Zool. *246:*156–170.

Hanken, J., and C.H. Summers (1988b) Developmental basis of evolutionary success: cranial ontogeny in a direct-developing anuran. Am. Zool. *28:*12A.

Hanken, J., and R.J. Wassersug (1981) The visible skeleton. Funct. Photogr. *16:*22–26, 44.

Hanken, J., M.W. Klymkowsky, D.W. Seufert, and N.E. Ingebrigtsen (1990) Evolution of cranial patterning in anuran amphibians analyzed using whole-mount immunohistochemistry. Am. Zool. *30:*138A.

Hedges, S.B. (1989) Evolution and biogeography of West Indian frogs of the genus *Eleutherodactylus:* slow-evolving loci and the major groups. In C.A. Woods (ed): Biogeography of the West Indies: Past, Present, and Future. Gainesville: Sandhill Crane Press, pp. 305–370.

Heyer, W.R. (1975) A preliminary analysis of the intergeneric relationships of the frog family Leptodactylidae. Smithsonian Contrib. Zool. No. 199:1–55.

Hughes, A. (1959) Studies in embryonic and larval development in Amphibia. I. The embryology of *Eleutherodactylus ricordii*, with special reference to the spinal cord. J. Embryol. Exp. Morphol. *7:*22–38.

Hughes, A. (1965) The development of behaviour in the embryo of *Eleutherodactylus martinicensis* (Amphibia, Anura). Proc. Zool. Soc. Lond. *144:*153–161.

Hughes, A. (1966) Spontaneous movements in the embryo of *Eleutherodactylus martinicensis*. Nature *211:* 51–53.

Humason, G.L. (1979) Animal Tissue Techniques, 4th ed. San Francisco: W.H. Freeman and Co.

Infantino, R.L., W.W. Burggren, and D.S. Townsend (1988) Physiology of direct development in the Puerto Rican frog *Eleutherodactylus coqui*. Am. Zool. *28:*23A.

Klymkowsky, M.W., and J. Hanken (1991) Whole-mount staining of *Xenopus* and other vertebrates. In B.K. Kay and H.B. Peng (eds): *Xenopus laevis:* Practical Uses in Cell and Molecular Biology. Methods in Cell Biology, Vol. 36 (in press).

Lauder, G.V., and K.F. Liem (1989) The role of historical factors in the evolution of complex organismal functions. In D.B. Wake and G. Roth (eds): Complex Organismal Functions: Integration and Evolution in Vertebrates. Chichester: John Wiley & Sons, Ltd., pp. 63–78.

Linsenmayer, T.F., and M.J.C. Hendrix (1980) Monoclonal antibodies to connective tissue macromolecules: type II collagen. Biochem. Biophys. Res. Commun. *92:*440–446.

Lombard, R.E., and D.B. Wake (1986) Tongue evolution in the lungless salamanders, family Plethodontidae. IV. Phylogeny of plethodontid salamanders and the evolution of feeding dynamics. Syst. Zool. *35:*532–551.

Lutz, B. (1947) Trends towards non-aquatic and direct development in frogs. Copeia *1947:*242–252.

Lutz, B. (1948) Ontogenetic evolution in frogs. Evolution *2:*29–39.

Lynch, J.D. (1971) Evolutionary relationships, osteology, and zoogeography of leptodactyloid frogs. Univ. Kans. Mus. Nat. Hist., Misc. Publ. No. 53:1–238.

Lynn, W.G. (1942) The embryology of *Eleutherodactylus nubicola,* an anuran which has no tadpole stage. Contrib. Embryol. Carnegie Inst. Wash. Publ. *541:*27–62.

Lynn, W.G. (1961) Types of amphibian metamorphosis. Am. Zool. *1:*151–161.

Lynn, W.G., and B. Lutz (1946) The development of *Eleutherodactylus guentheri* Stdnr. 1864. Bol. Mus. Nac. Zool. *71:*1–46.

McDiarmid, R.W. (1978) Evolution of parental care in frogs. In G.M. Burghardt and M. Bekoff (eds): The Development of Behavior: Comparative and Evolutionary Aspects. New York: Garland STPM Press.

Orton, G.L. (1951) Direct development in frogs. Turtox News *29:*2–6.

Parks, A.L., B.A. Parr, J.-E. Chin, D.S. Leaf, and R.A. Raff (1988) Molecular analysis of heterochronic changes in the evolution of direct developing sea urchins. J. Evol. Biol. *1:*27–44.

Raff, R.A. (1987) Constraint, flexibility, and phylogenetic history in the evolution of direct development in sea urchins. Dev. Biol. *119:*6–19.

Raff, R.A., and G.A. Wray (1989) Heterochrony: developmental mechanisms and evolutionary results. J. Evol. Biol. *2:*409–434.

Roth, G., and D.B. Wake (1985) Trends in the functional morphology and sensorimotor control of feeding behavior in salamanders: an example of the role of internal dynamics in evolution. Acta Biotheor. (Leiden) *34:*175–192.

Roth, G., and D.B. Wake (1989) Conservatism and innovation in the evolution of feeding in vertebrates. In D.B. Wake and G. Roth (eds): Complex Organismal

Functions: Integration and Evolution in Vertebrates. Chichester: John Wiley & Sons, Ltd., pp. 7–21.

Sedra, S.N. (1950) The metamorphosis of the jaws and their muscles in the toad, *Bufo regularis* Reuss, correlated with the changes in the animal's feeding habits. Proc. Zool. Soc. Lond. *120:*405–449.

Strathmann, R.R. (1988) Larvae, phylogeny, and von Baer's law. In C.R.C. Paul and A.B. Smith (eds): Echinoderm Phylogeny and Evolutionary Biology. Oxford: Clarendon Press, pp. 53–68.

Taigen, T.L., F.H. Pough, and M.M. Stewart (1984) Water balance of terrestrial anuran (*Eleutherodactylus coqui*) eggs: importance of parental care. Ecology *65:* 248–255.

Townsend, D.S., and M.M. Stewart (1985) Direct development in *Eleutherodactylus coqui* (Anuran: Leptodactylidae): a staging table. Copeia *1985:*423–436.

Trueb, L. (1985) A summary of osteocranial development in anurans with notes on the sequence of cranial ossification in *Rhinophrynus dorsalis* (Anura: Pipoidea: Rhinophrynidae). S. Afr. J. Sci. *81:*181–185.

Wake, D.B. (1982) Functional and developmental constraints and opportunities in the evolution of feeding systems in urodeles. In D. Mossakowski and G. Roth (eds): Environmental Adaptation and Evolution. Stuttgart: Gustav Fischer, pp. 51–66.

Wake, D.B., and G. Roth (1989) The linkage between ontogeny and phylogeny in the evolution of complex systems. In D.B. Wake and G. Roth (eds): Complex Organismal Functions: Integration and Evolution in Vertebrates. Chichester: John Wiley & Sons, Ltd., pp. 361–377.

Wake, D.B., K.C. Nishikawa, U. Dicke, and G. Roth (1988) Organization of the motor nuclei in the cervical spinal cord of salamanders. J. Comp. Neurol. *278:*195–208.

Wake, M.H. (1989) Phylogenesis of direct development and viviparity in vertebrates. In D.B. Wake and G. Roth (eds): Complex Organismal Functions: Integration and Evolution in Vertebrates. Chichester: John Wiley & Sons, Ltd., pp. 235–250.

Wake, M.H., and J. Hanken (1982) The development of the skull of *Dermophis mexicanus* (Amphibia: Gymnophiona), with comments on skull kinesis and amphibian relationships. J. Morphol. *173:*203–223.

Wassersug, R.J., and K. Hoff (1982) Developmental changes in the orientation of the anuran jaw suspension. Evol. Biol. *15:*223–246.

Wiens, J.J. (1989) Ontogeny of the skeleton of *Spea bombifrons* (Anura: Pelobatidae). J. Morphol. *202:*29–51.

Wray, G.A., and D.R. McClay (1989) Molecular heterochronies and heterotopies in early echiniod development. Evolution *43:*803–813.

Wray, G.A., and R.A. Raff (1989) Evolutionary modification of cell lineage in the direct-developing sea urchin *Heliocidaris erythrogramma.* Dev. Biol. *132:*458–470.